Computational Materials Science 81 (2014) 524–529

Contents lists available at ScienceDirect

Computational Materials Science

journal homepage: www.elsevier.com/locate/commatsci

Structure and thermomechanical behavior of bent GaN nanowires

Kwangsub Jung [a], Maenghyo Cho [b], Min Zhou [b,c,*]

[a] Quality and Reliability Team, System LSI Business, Samsung Electronics Co., Ltd., Yongin 446-811, South Korea
[b] WCU Program on Multiscale Mechanical Design, School of Mechanical and Aerospace Engineering, Seoul National University, Seoul 151-742, South Korea
[c] George W. Woodruff School of Mechanical Engineering, School of Materials Science and Engineering, Georgia Institute of Technology, Atlanta, GA 30332-0405, USA

ARTICLE INFO

Article history:
Received 10 June 2013
Received in revised form 28 August 2013
Accepted 3 September 2013
Available online 30 September 2013

Keywords:
GaN nanowires
Thermal conductivity
Molecular dynamics
Phase transformation

ABSTRACT

The thermal and mechanical behaviors of bent GaN nanowires are investigated using molecular dynamics (MD) simulations. The nanowires considered have an axial orientation along the [0001] crystalline direction and hexagonal cross sections with diameters of 2.91 and 3.55 nm. A phase transformation from wurtzite to a tetragonal structure occurs near the surfaces of the nanowires in the bending process. The thermal conductivity is evaluated using an analytical model. This model is based on the same atomistic potential used in the MD calculations and uses configurational information from the MD calculations as input. The method is 50 times more computationally efficient compared with the Green–Kubo method. It is found that the thermal conductivity decreases by 35% and 25%, respectively, for nanowires 2.91 and 3.55 nm in diameter during the phase transformation in the bending process. In contrast, the thermal conductivity does not change during unloading and is found to be independent of the bending angle. The overall trend in thermal and mechanical responses of the nanowire with a diameter of 3.55 nm is similar to that for the nanowire with a diameter of 2.91 nm. Results also show that the phase transformation due to bending cannot be reversed by simple unloading. The finding points out a mechanism for altering the structure and thermal conductivity of GaN nanowires through transverse mechanical loading.

1. Introduction

Flexible electronic devices have attracted significant interest from both industry and the academic research community. Designs with significant flexibility can improve mobility, portability, functionality and convenience of devices [1–7]. Flexible nanostructures have many potential applications, including wearable computers, paper displays, and flexible solar cells [8–11]. The integration of nanomaterials can provide a new framework for the development of flexible nanoelectronic devices and self-powered nanosystems [12]. For example, ZnO nanowire arrays vertically aligned on a substrate have been used to generate electricity. During the operation of flexible devices, external loading can change the structures of nanomaterials, leading to simultaneous changes in physical properties. Coupled changes in thermal and mechanical behaviors in GaN and ZnO nanowires during tensile loading and unloading have been extensively investigated [13–15]. These studies are motivated by the fact that tensile loading of [0001] nanowires causes a phase transformation from the wurtzite (WZ) to a tetragonal structure (TS) which is reversible upon unloading [15]. Transitional states observed during the transformation include combined WZ–TS structures and an inversion domain boundary (IDB) [16]. Studies have also shown that the thermal conductivity of GaN nanowires depends on strain, structure, and size. The thermal conductivity decreases as strain increases under loading and increases as the strain decreases in the unloading process. The thermal conductivities of the nanowires in the intermediate states of the reverse transformation are lower than those of WZ-structured nanowires at the same strain.

Previous studies usually assume that nanowires are straight and external force is along the axis [17–19]. However, nanowires and nanofilms are not always perfectly straight. They are often bent in fabrication and operation. The influence of bending deformation on the thermal conductivity has been investigated for dielectric nanowires [20], carbon nanotubes [21] and graphene sheets [22]. Liu et al. [20] used phonon transport Monte Carlo simulations to show that curvature reduces the thermal conductivity of Si nanowires. Non-equilibrium MD simulations have also been used in the analysis of carbon nanotubes and graphene sheets. Zhong et al. [21] showed that the thermal conductivity of carbon nanotubes does not change with bending angle. The graphene sheets keep their high thermal conductivity even at high curvatures [22]. For GaN nanowires, phase transformation can occur during bending because bending deformation is associated with both

* Corresponding author at: George W. Woodruff School of Mechanical Engineering, School of Materials Science and Engineering, Georgia Institute of Technology, Atlanta, GA 30332-0405, USA. Tel.: +1 404 894 3294; fax: +1 404 894 0186.
E-mail address: min.zhou@gatech.edu (M. Zhou).

0927-0256/$ - see front matter © 2013 Elsevier B.V. All rights reserved.
http://dx.doi.org/10.1016/j.commatsci.2013.09.008

tension and compression in the nanowire. In this study, the phase transformation of WZ-structured GaN nanowires in response to bending deformation is analyzed and relevant thermal and mechanical behaviors are investigated. In the design of flexible and self-powered nanodevices, bending deformation of piezoelectric nanowires is often desired for power generation [12]. The bending behaviors of nanostructures are different from the behaviors under axial loading because bending involves both tension and compression. Here in this paper, we focus on the thermal and mechanical responses of nanowires during bending and recovery from the bent configuration. The investigation of the thermomechanical responses of bent [0001]-oriented GaN nanowires uses molecular dynamics (MD) computations and an analytical model developed recently. Of particular interest are the phase transformation observed in the bending process and the change in thermal and mechanical behaviors. Comparison is made with the behaviors observed during axial loading and unloading.

2. Methods

The MD simulations are carried out using the LAMMPS package [23]. The Buckingham potential [24] and the Wolf summation [25,26] are used to describe the interactions between atoms in the MD simulations. For bulk GaN, the volumes per two Ga-N pairs for unstressed WZ and TS structures are 47.1 Å^3 and 49.5 Å^3, respectively. For unstressed GaN, WZ is the most stable structure with lower energy, with the energy difference between WZ and TS being 0.068 eV/atom. However, at a strain of 0.08 the TS structure is more stable than the WZ structure, with the energy of TS being 0.017 eV/atom lower than that of WZ. The GaN nanowires analyzed have a hexagonal cross section and the WZ structure with a sixfold symmetry around the [0001] axis, as shown in Fig. 1 of Ref. [15]. The wires considered have diameters of 2.91 and 3.55 nm. Boundary conditions are periodic in the axial direction and lateral surfaces of the wires are traction-free. The atomic structure in the computational cell is a part of a nanowire with infinite length, as illustrated in Fig. 1. The nanowires are equilibrated for 200 ps before bending deformation. Stress in the wire is maintained at zero using the NPT (isothermal-isobaric ensemble) algorithm [27] along the axial direction. The combination of the periodic boundary condition and NPT algorithm enables the cell to stretch or shrink in length. A quasi-static loading scheme is used to analyze the deformation. After the 200 ps equilibration, atoms in the middle of the nanowire are forced to move by 0.01 nm in the transverse $[01\bar{1}0]$ direction. The nanowires are then equilibrated for another 200 ps. During this equilibration process, boundary conditions are imposed on the moved atoms in the transverse direction by placing relevant atoms on transverse supports, such that the overall bent configuration is maintained while internal changes can occur, if the conditions so dictate. The boundary conditions restrict the movement of supported atoms in the direction of the deflection. Unloading of the bent nanowires is carried out in a manner similar to that for the loading process. The one-direction NPT algorithm is also used during the equilibration periods between bending or unloading time steps. As illustrated in Fig. 2, the flexure of the nanowire is characterized by the bending angle θ in the form of:

$$\theta = \tan^{-1}\left(\frac{\delta}{L/2}\right), \tag{1}$$

where δ is the deflection of nanowire and L is the length of the simulation cell.

The thermal conductivity in the axial direction is evaluated using a model based on the atomistic potential developed recently [28]. The model uses atomistic configurational information and interatomic interactions to calculate the thermal conductivity κ through

$$\kappa = \kappa_0 \left[\frac{V_2(\varepsilon)}{V_2(0)}\right]^a \left[\frac{V_3(\varepsilon)}{V_3(0)}\right]^b, \tag{2}$$

where κ_0 is the thermal conductivity of the undeformed structure; $V_2(\varepsilon)$ and $V_3(\varepsilon)$ are second-order and third-order force constants at strain ε, respectively; and a and b are model parameters. The

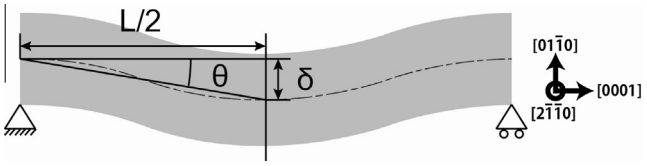

Fig. 2. The bending angle calculated based on the length of the simulation cell and the deflection of the nanowire.

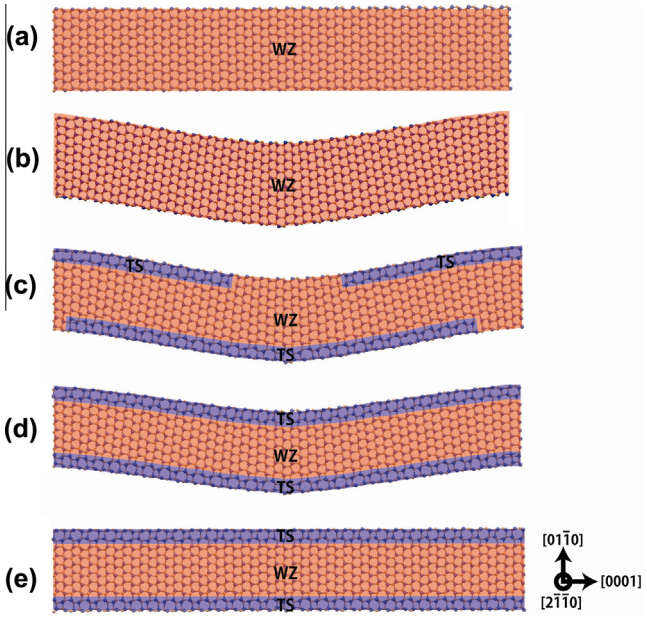

Fig. 3. Arrangement of atoms on $(2\bar{1}\bar{1}0)$ sections of a nanowire with $d = 2.91$ nm in the processes of bending and unloading: (a) WZ-structured wire at $\theta = 0$; (b) WZ-structured wire at $\theta = 7.8^\circ$ in the bending process; (c) TS–WZ structured wire at $\theta = 8.3^\circ$ in the bending process; (d) TS–WZ structured wire at $\theta = 7.5^\circ$ in the unloading process; and (e) straight, TS–WZ structured wire at $\theta = 0$ at the end of unloading. The blue regions indicate TS structures.

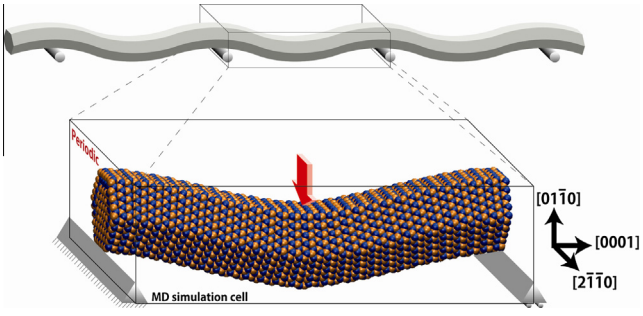

Fig. 1. A schematic view of a bent GaN nanowire with the wurtzite structure and a hexagonal cross section. Periodic boundary conditions are used along the axis of the nanowire.

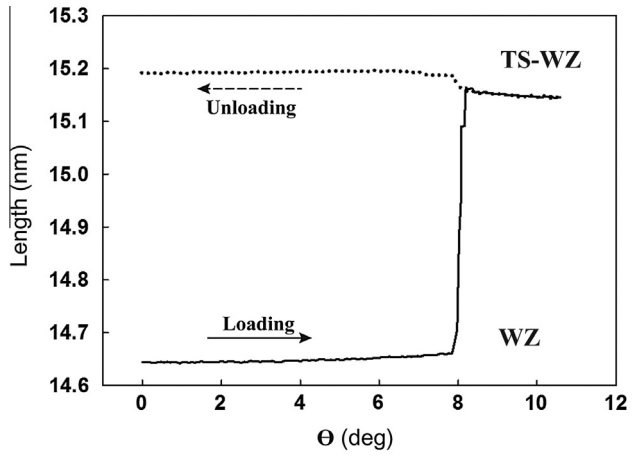

Fig. 4. Length of a nanowire as a function of bending angle.

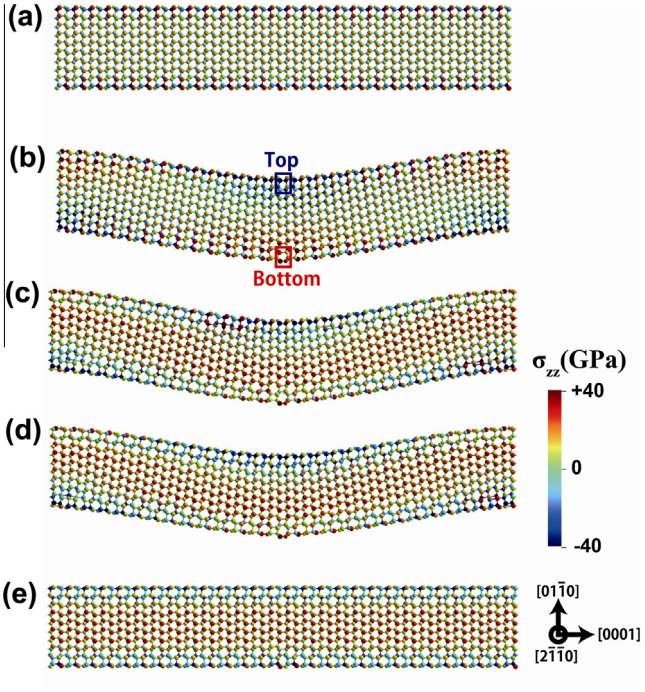

Fig. 5. Stress on atoms on $(2\bar{1}\bar{1}0)$ sections of a nanowire with $d = 2.91$ nm in the processes of bending and unloading: (a) WZ-structured wire at $\theta = 0$; (b) WZ-structured wire at $\theta = 7.8^\circ$ in the bending process; (c) TS–WZ structured wire at $\theta = 8.3^\circ$ in the bending process; (d) TS–WZ structured wire at $\theta = 7.5^\circ$ in the unloading process; and (e) straight, TS–WZ structured wire with $\theta = 0$ at the end of the unloading process.

thermal responses obtained using this model are consistent with the results obtained from Green–Kubo MD calculations [15,29–31]. This model, approximately 50 times more computationally efficient than the Green–Kubo method, has been used to predict the dependence of thermal conductivity on strain and atomistic structure of the GaN nanowires under axial loading [15]. To evaluate the thermal conductivity, the second-order and third-order force constants at each deformed state are calculated based on the atomic configurations obtained from the MD simulations of the bending process. The computational cost for the thermal conductivity calculation using the Green–Kubo method is fifty times that for the mechanical response calculation [15]. Details of the model are given in Ref. [28]. Temperature is kept constant at 300 K using the

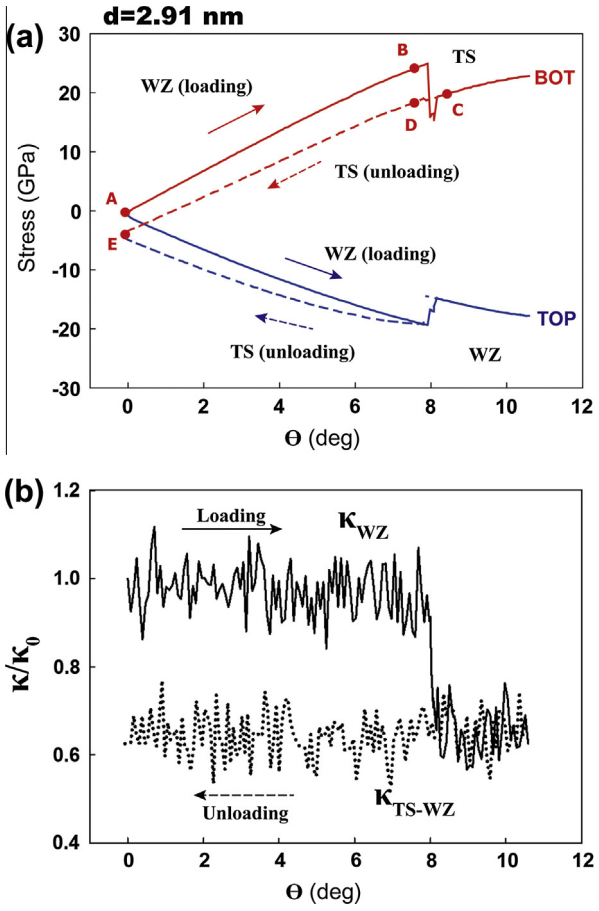

Fig. 6. (a) Stress in the bottom and top regions as functions of bending angle for a GaN nanowire with diameter $d = 2.91$ nm. (b) Thermal conductivity as a function of bending angle for the same nanowire.

Nosé–Hoover algorithm [32]. This is the value of temperature after quantum correction [14,33]. The overall stress is calculated according the atomistic stress formula [34].

3. Results

3.1. Mechanical responses

The mechanical behavior of nanowires with a diameter of 2.91 nm is analyzed first. As the deflection and bending angle increase, the WZ-structured nanowire deforms, as shown in Fig. 3. When the bending angle approaches 8.0°, the WZ structure of atoms on the surfaces transforms into the TS structure, as indicated by blue regions in Fig. 3. This phase transformation on the surfaces is similar to the transformations observed in ZnO and GaN nanowires under tensile loading [14,15,35–38]. The relative favorability of the two phases is studied by calculating the enthalpy using the density functional theory [35,38]. The WZ–TS reconstruction in ZnO is recently observed in experiments [39]. In contrast to what is observed in the same nanowire under axial loading, phase transformation is not observed in the interior, as can be seen in Fig. 3. As shown in Fig. 4, the length of the wire remains essentially unchanged before the phase transformation. When the WZ-to-TS transformation occurs, the length of the nanowire increases from its initial value of 14.6 nm by 3%. The lattice constant for the unstressed TS ZnO along the [0001] axis is 7% larger than that for the WZ ZnO [35]. The lattice constants for the TS GaN have not been reported, but the c/a lattice ratios of WZ, hexagonal, and

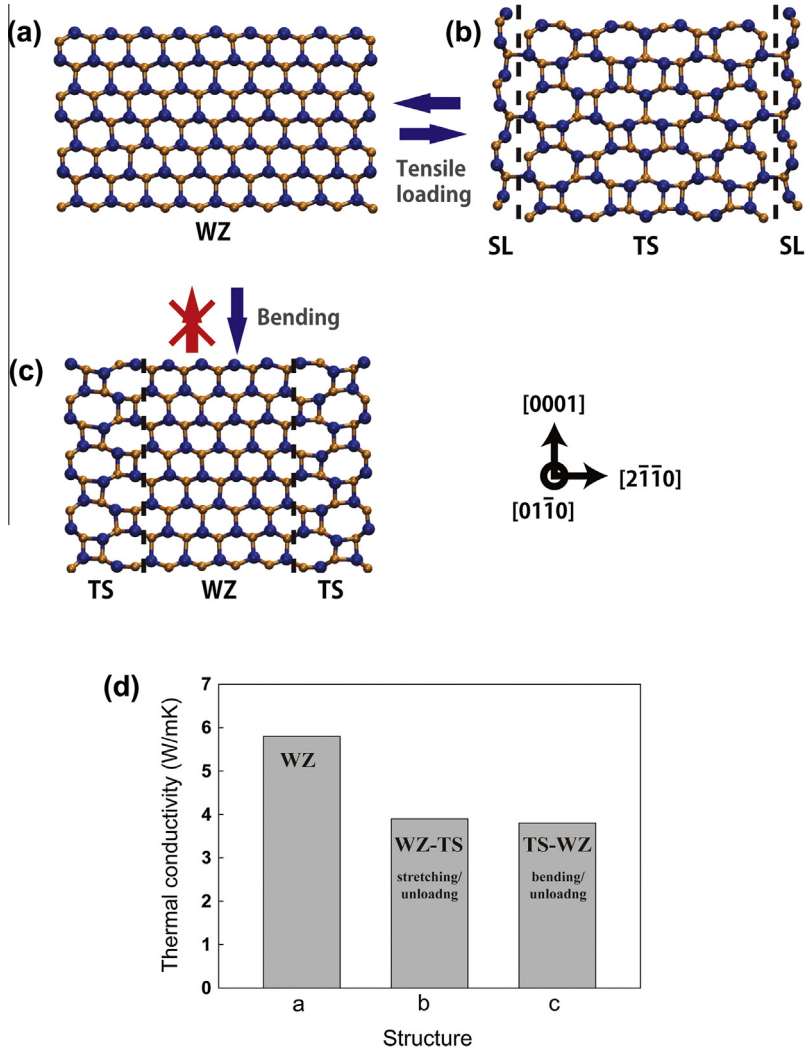

Fig. 7. Atomistic arrangements on $(0\,1\,\bar{1}\,0)$ cross-sections of a GaN nanowire with $d = 2.91$ nm: (a) unstressed WZ-structured nanowire; (b) TS-structured nanowire with surface layers (SL) under tensile loading; (c) TS–WZ structured nanowire during bending; (d) Thermal conductivities of the unstressed WZ-structured nanowire, WZ–TS structured nanowire in the process of unloading with strain, and TS–WZ structured nanowires in the process of unloading.

rocksalt structures are very similar for SiC, InN, CdSe, ZnO, and GaN because they have the same WZ structure under ambient conditions and show the same phase transformation under external stress [40]. The c/a ratio of the rocksalt structure is 1 because a is equal to c, as illustrated in Fig. 1 of Ref. [40]. The ratio is listed only for comparison with other structures. The phase transformation from WZ to TS is observed in the nanowires under tensile loading. Here, the axial stress of the bent nanowire is maintained at zero. The NPT algorithm controls only the sum of stresses for all atoms in the nanowire. At the individual atom level, the stress for each atom is not necessarily zero. The bent nanowires consist of both stretched and compressed regions, as seen in Fig. 5. At a bending angle of $\theta = 7.8^\circ$, tensile stresses act on atoms in the bottom region outlined by the red[1] square, and compressive stresses act on atoms in the top region outlined by the blue square in Fig. 5. Fig. 6(a) shows the stresses in both regions as functions of the bending angle. The stress in the bottom region increases along the solid red line in Fig. 6(a) as the bending angle increases from zero to 8.0°. When the WZ structure on the surfaces transforms into the TS structure at the bending angle of $\theta = 8.0^\circ$, the stress in the bottom region drops. This drop is also shown in the change in stress in bottom region in Fig. 5(b) and (c). The relation between the stress and the bending angle is similar to the stress–strain relation for the nanowire under tensile loading in Ref. [15]. The TS structure is observed first in the bottom and spreads to 90% of the surface regions at a bending angle of $\theta = 8.3^\circ$. The nanowire deforms in the TS–WZ structure until it breaks into two parts at a bending angle of $\theta = 11.1^\circ$. The fracture occurs in the middle of the nanowire. The initial WZ structure remains in the interior and top region, as seen in Fig. 3(c). Unloading from the bending angle of $\theta = 10.5^\circ$ is also analyzed. When the bending angle decreases to 7.5°, the WZ structure which remains in 10% of the surface regions transforms into the TS structure, as shown in Fig. 3(d). The nanowire deforms in the TS–WZ structure throughout the unloading process. As a result of the loading/unloading deformation process, the straight nanowire ($\theta = 0$) at the end has the TS structure in areas close to its surfaces. The reverse transformation from TS to WZ is not observed. The red dashed line and the blue dashed line in Fig. 6(a) indicate the relation between the stress and the bending angle in the unloading process. The stress in the bottom region does not show an abrupt change because the atomistic structure there does not change in the unloading process. For axial loading and unloading, the WZ-structured nanowires transform into the TS structure under tensile loading and re-

[1] For interpretation of color in Figs. 5 and 6, the reader is referred to the web version of this article.

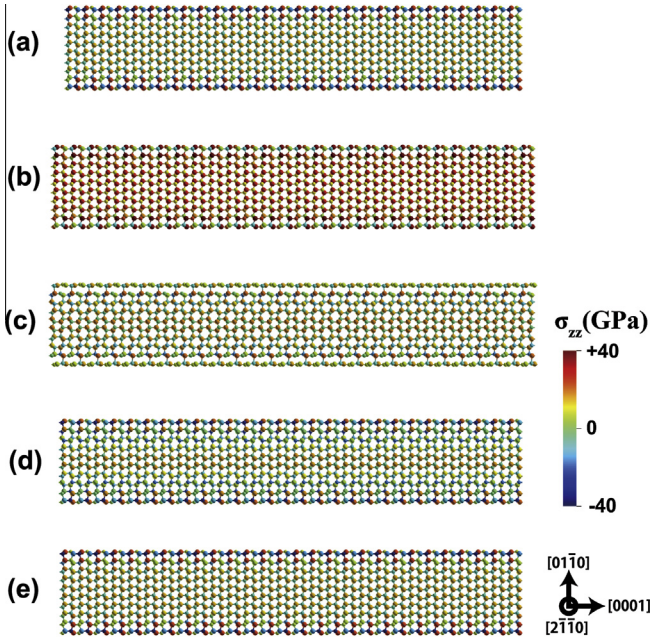

Fig. 8. Stress on atoms on $(2\bar{1}\bar{1}0)$ sections of a nanowire with $d = 2.91$ nm during tensile loading and unloading: (a) WZ-structured wire at zero strain; (b) WZ-structured wire at a strain of 0.06 under loading; (c) TS-structured wire at a strain of 0.07 after the WZ-to-TS transformation under loading; (d) WZ–TS structured wire at zero strain before the completion of the TS-to-WZ transformation in the unloading process and (e) WZ-structured wire at zero strain after the reverse transformation in the unloading process.

vert to the WZ structure during unloading [15], as illustrated in Fig. 7. The interatomic potential and the dimensions and geometry of the nanowires used in the previous work on axial loading and unloading [15] are the same as those used in this work. In contrast, such a reverse transformation is not observed for bending. The differences in the structural changes are attributed to internal stresses in the nanowires. As shown in Fig. 8, all atoms of the stretched nanowire are under tensile stress before the WZ-to-TS transformation and the tensile stresses disappear after the transformation. This is also indicated by the stress drop in Fig. 2 of Ref. [15]. Similarly, the completion of the TS-to-WZ transformation is associated with the vanishing of the compressive stress. The critical stress required for the initiation of the TS-to-WZ transformation indicated in Fig. 2(a) of Ref. [15] is −3.1 GPa. This value is the sum of the stresses for all atoms. The stress in the TS regions in Fig. 8(d) is −7.0 GPa before the reverse transformation. This is very close to the critical stress for the TS-to-WZ transformation of bulk GaN [15]. As shown in Fig. 6(a), the stress in the bottom region decreases as the bending angle decreases during unloading. The stress at point E ($\theta = 0$) in Fig. 6(a) is −3.4 GPa. This compression on atoms is not enough for the initiation of the TS-to-WZ transformation. For the top surface regions, the TS structure does not transform into the WZ structure because the magnitude of compressive stress decreases in the unloading process. Therefore, no reverse phase transformation occurs in the bent nanowires anywhere during unloading.

3.2. Thermal responses

The thermal behavior of the nanowire with a diameter of $d = 2.91$ nm is also investigated. Fig. 6(b) shows the thermal conductivity as a function of bending angle for the nanowire in Fig. 6(a). The thermal conductivity of the WZ-structured nanowires is largely constant for bending angle values up to 8.0°. When the structural change occurs in the surface regions at

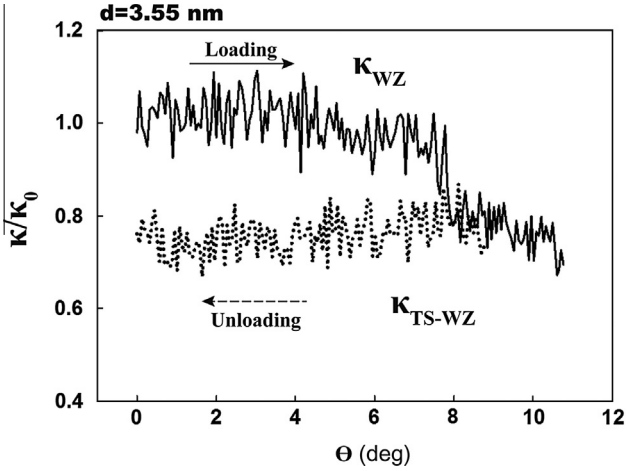

Fig. 9. Thermal conductivity as a function of bending angle for a GaN nanowire with a diameter $d = 3.55$ nm.

$\theta = 8.0°$, the thermal conductivity drops precipitously. Thermal conductivity of the TS–WZ structured nanowires is 3.8 W/mK or approximately 65% that of the WZ-structured nanowires. Such a lower thermal conductivity of nanowires with a heterogeneous structure is also predicted for the nanowires in the stretching/unloading process [15]. The thermal conductivity of WZ–TS structured nanowires with the same diameter ($d = 2.91$ nm) in the unloading process is 3.9 W/mK, or 33% lower than that for the homogeneous WZ nanowires. This dependence of thermal conductivity on atomistic structure is attributed to the dependence of the stiffness of the nanowire on structure. The effect of structure on the thermal conductivity comes from the phonon group velocity which is related to the stiffness of the nanowire [41,42]. Specifically, the elastic moduli of the WZ and WZ–TS structured nanowires are 318.8 and 242.7 GPa, respectively [15]. For the bending/unloading process, the elastic modulus of the TS–WZ structured nanowires is 243.3 GPa, which is very close to that for the WZ–TS nanowires during stretching/unloading. The strain effects on thermal conductivity are also significant for the nanowires in the stretching/unloading process. The thermal conductivity decreases as the strain increases under tensile loading, and increases as the strain decreases under compressive loading. However, the thermal conductivity of the bent nanowires remains essentially unchanged as the bending angle changes. Before the phase transformation, the thermal conductivity is rather independent of the curvature of the wires' bending curve. The strain effects observed in axially loaded wires are absent from the bent nanowires. In the unloading process, thermal conductivity does not change with the bending deformation because no phase transformation occurs. Consequently, the thermal conductivity of straight TS–WZ structured nanowires at the end of unloading is 33% lower than that of the WZ-structured nanowires. Unloading of the bent nanowires does not change the thermal conductivity because the no structural change is associated with the unloading process. Here, the dependence of thermal conductivity on structure is more pronounced because strain effects are absent in the bent nanowires.

Fig. 9 shows the thermal conductivity as a function of the bending angle for the nanowire with a diameter of $d = 3.55$ nm. The overall trend is similar to that for the nanowire with the smaller diameter in Fig. 6. The phase transformation near the surfaces of the nanowire lowers thermal conductivity by 25% at a bending angle of $\theta = 8.0°$ during loading. In the unloading process, the thermal conductivity does not change with the bending angle, as seen in Fig. 6 as well.

4. Summary

The thermomechanical behaviors of bent [0001]-oriented GaN nanowires with diameters of 2.91 and 3.55 nm are investigated using molecular dynamics simulations and a new analytical model. The WZ structure near the surfaces of the nanowires transforms into the TS structure during bending. This structural change results from the internal stresses in nanowires. The bent nanowires consist of regions under tensile stresses and regions under compressive stresses. The phase transformation from WZ to TS initiates from the tension regions on surface and spreads to most of surfaces. The phase transformation is not reversed and the TS structure on the surfaces remains during unloading of bent nanowires. This phenomenon is in contrast to what is observed in the same nanowires under axial loading and unloading where the phase transformation reverses spontaneously upon unloading. Analysis reveals that the reason for the difference is because the stress conditions in the bent wire are different from those in the axially loaded wires. The observed structural changes have significant influences on the thermal behaviors of bent nanowires. In particular, the thermal conductivity of the nanowire depends on the structure and size of the nanowires. The thermal conductivity of the TS–WZ nanowires is 35% and 25% lower than those of the WZ-structured nanowires, respectively, for the diameters of 2.91 and 3.55 nm. This effect of structure is attributed to the mechanical behaviors of nanowires. Specifically, the decrease in the elastic modulus of TS–WZ structured nanowires relative to that of the WZ-structured wires lowers the thermal conductivity by reducing the phonon group velocity. The thermal conductivity decreases during the phase transformation on the surfaces in the bending process, and does not change in the unloading process. The thermal conductivity is independent of the bending angle because of the absence of the strain effect. Straight, unstressed GaN nanowires can have two different structural regions as a result of bending and subsequent unbending. These results point out a mechanism which can be used to control the thermal and mechanical properties of nanostructures.

Acknowledgment

The authors gratefully acknowledge support from the National Research Foundation of Korea through Grant No. R31-2011-000-10083-0 and Grant No. 2012R1A3A2048841 at Seoul National University.

References

[1] P.X. Gao, J. Song, J. Liu, Z.L. Wang, Adv. Mater. 19 (2007) 67–72.
[2] M.Y. Choi, D. Choi, M.J. Jin, I. Kim, S.H. Kim, J.Y. Choi, S.Y. Lee, J.M. Kim, S.W. Kim, Adv. Mater. 21 (2009) 2185–2189.
[3] Z. Li, R. Zhang, K.S. Moon, Y. Liu, K. Hansen, T. Le, C.P. Wong, Adv. Funct. Mater. 23 (2013) 1459–1465.
[4] K. Nomura, H. Ohta, A. Takagi, T. Kamiya, M. Hirano, H. Hosono, Nature 432 (2004) 488–492.
[5] H.E.A. Huitema, G.H. Gelinck, J.B.P.H. van der Putten, K.E. Kuijk, C.M. Hart, E. Cantatore, P.T. Herwig, A.J.J.M. van Breemen, D.M. de Leeuw, Nature 414 (2001) 599.
[6] D.B. Mitzi, L.L. Kosbar, C.E. Murray, M. Copel, A. Afzali, Nature 428 (2004) 299–303.
[7] D.H. Kim, J.A. Rogers, Adv. Mater. 20 (2008) 4887–4892.
[8] T. Starner, IBM Syst. J. 35 (1996) 618–629.
[9] T. Starner, S. Mann, B. Rhodes, J. Levine, J. Healey, D. Kirsch, R.W. Picard, A. Pentland, Presence 6 (1997) 386–398.
[10] T.W. Kelley, P.F. Baude, C. Gerlach, D.E. Ender, D. Muyres, M.A. Haase, D.E. Vogel, S.D. Theiss, Chem. Mater. 16 (2004) 4413–4422.
[11] F.C. Krebs, S.A. Gevorgyan, J. Alstrup, J. Mater. Chem. 19 (2009) 5442–5451.
[12] G. Zhu, R. Yang, S. Wang, Z.L. Wang, Nano Lett. 10 (2010) 3151–3155.
[13] A.J. Kulkarni, M. Zhou, Nanotechnology 18 (2007) 435706.
[14] K. Jung, M. Cho, M. Zhou, Appl. Phys. Lett. 98 (2011) 041909.
[15] K. Jung, M. Cho, M. Zhou, J. Appl. Phys. 112 (2012) 083522.
[16] P. Xiao, X. Wang, J. Wang, F. Ke, M. Zhou, Y. Bai, Appl. Phys. Lett. 95 (2009) 211907.
[17] Y.R. Chen, M.S. Jeng, Y.W. Chou, C.C. Yang, Comput. Mater. Sci. 50 (2011) 1932–1936.
[18] S.P. Ju, M.H. Weng, W.J. Lee, J.S. Lin, Comput. Mater. Sci. 42 (2008) 595–599.
[19] J. Wang, W. Hu, X. Li, S. Xiao, H. Deng, Comput. Mater. Sci. 50 (2010) 373–377.
[20] L.C. Liu, M.J. Huang, R. Yang, M.S. Jeng, C.C. Yang, J. Appl. Phys. 105 (2009) 104313.
[21] W.R. Zhong, M.P. Zhang, D.Q. Zheng, B.Q. Ai, J. Appl. Phys. 109 (2011) 074317.
[22] B. Mortazavi, A. Rajabpour, S. Ahzi, Y. Rémond, S.M.V. Allaei, Solid State Commun. 152 (2012) 261–264.
[23] S.J. Plimpton, J. Comput. Phys. 117 (1995) 1–19.
[24] P. Zapol, R. Pandey, J.D. Gale, J. Phys.: Condens. Matter 9 (1997) 9517–9525.
[25] D. Wolf, P. Keblinski, S.R. Phillpot, J. Eggebrecht, J. Chem. Phys. 110 (1999) 8254–8282.
[26] C.J. Fennell, J.D. Gezelter, J. Chem. Phys. 124 (2006) 234104.
[27] G.J. Martyna, D.J. Tobias, M.L. Klein, J. Chem. Phys. 101 (1994) 4177–4189.
[28] K. Jung, M. Cho, M. Zhou, AIP Advances 3 (2013) 072123.
[29] S.G. Volz, G. Chen, Phys. Rev. B 61 (2000) 2651–2656.
[30] A.J.H. McGaughey, M. Kaviany, Int. J. Heat Mass Transfer 47 (2004) 1783–1798.
[31] A.J.H. McGaughey, M. Kaviany, Int. J. Heat Mass Transfer 47 (2004) 1799–1816.
[32] W.G. Hoover, Phys. Rev. A 31 (1985) 1695–1697.
[33] Y.H. Lee, R. Biswas, C.M. Soukoulis, C.Z. Wang, C.T. Chan, K.M. Ho, Phys. Rev. B 43 (1991) 6573–6580.
[34] M. Zhou, Proc. R. Soc. London A 459 (2003) 2347–2392.
[35] J. Wang, A.J. Kulkarni, K. Sarasamak, S. Limpijumnong, M. Zhou, Phys. Rev. B 76 (2007) 172103.
[36] J. Wang, A.J. Kulkarni, F.J. Ke, Y.L. Bai, M. Zhou, Comput. Methods Appl. Mech. Eng. 197 (2008) 3182–3189.
[37] J. Wang, P. Xiao, M. Zhou, Z.R. Wang, F.J. Ke, J. Appl. Phys. 107 (2010) 023512.
[38] A.J. Kulkarni, K. Sarasamak, J. Wang, F.J. Ke, S. Limpijumnong, M. Zhou, Mech. Res. Commun. 35 (2008) 73–80.
[39] M.R. He, R. Yu, J. Zhu, Angew. Chem. 124 (2012) 7864–7867.
[40] K. Sarasamak, A.J. Kulkarni, M. Zhou, S. Limpijumnong, Phys. Rev. B 77 (2008) 024104.
[41] A.J. Kulkarni, M. Zhou, Appl. Phys. Lett. 88 (2006) 141921.
[42] A.J. Kulkarni, M. Zhou, Acta Mech. Sin. 22 (2006) 217–224.